Acetylene absorption by ionic liquids: A multiscale analysis based on molecular and process simulation

R. Santiago, J. Bedia, D. Moreno, C. Moya, J. de Riva, M. Larriba, J. Palomar*

Sección de Ingeniería Química. Universidad Autónoma de Madrid. 28049 Madrid. Spain.

*Corresponding author. E-mail: pepe.palomar@uam.es

Keywords: Acetylene; Absorption; Ionic Liquids; COSMO-RS; Aspen Plus; ILUAM

Abstract

A COSMO-based/Aspen Plus multiscale simulation methodology was used to evaluate a wide variety of ionic liquids (ILs), more than 300, as potential acetylene absorbents. First, by means of Conductor-like-Screening Model for Real Solvents (COSMO-RS) method, molecular simulations were conducted to select ILs with adequate thermodynamic (Henry's law constants) and kinetic (diffusion coefficients) properties as acetylene absorbents, using N,N-dimethylformamide (DMF) as benchmark industrial solvent for such solute absorption. Then, the operating units of acetylene absorption of acetylene absorption from argon, and exhausted solvent regeneration were modeled in Aspen Plus. Simulations of absorption column using equilibrium based design model demonstrated that at least two ILs (1-butyl-3-methylimidazolium cation and acetate and sulfonate anions) present competitive solvent performance in acetylene absorption respect to DMF. In contrast, process analyses with a more realistic rate-based column model revealed that the mass transfer rate clearly controls the acetylene absorption with ILs compared to DMF, due to their viscosity differences. Finally, modeling solvent regeneration stage showed clear advantages of using ILs as acetylene absorbents since efficient acetylene recovery is achieved by flash distillation (vacuum pressure and temperature increase), operation hindered in the case of DMF due to is high volatility, requiring the solvent regeneration by a distillation equipment with higher operating and investment costs. Current COSMO-based/Aspen Plus approach has been demonstrated useful to perform preliminary analyses of the potential application of ILs in new separation processes, before starting with experimental essays, highly demanding in cost and time.

1. Introduction

Acetylene (C_2H_2) is an important organic raw material used in different industrial applications such as soldering or illumination and heat source [1]. The low yield of acetylene synthetized (between 5-30% of the total acetylene commercialized) in the chemical industry (by cracking naphtha or natural gas and plasma pyrolysis of coal) makes its separation and purification necessary [2]. The acetylene produced is accompanied with ethylene (C_2H_4), an essential chemical compound in the production of polymers such as polyethylene [3]. The presence of acetylene in the polymerization reactions of ethylene is undesired, since it can produce the catalyst poisoning influencing directly in the quality of the product [4]. Furthermore, during the polymerization reactions, an explosion can happen if acetylenic compounds are converted into solids and block the fluid stream. For these reasons, it is important to eliminate efficiently the acetylene from the ethylene feed streams [5]. The removal of acetylene from ethylene streams is commercially carried out by partial hydrogenation of acetylene over a supported noble metal catalyst such as Pd [6]. This process presents some disadvantages like the potential production of ethane by overhydrogenation of acetylene, causing the loss of the desirable reactive (ethylene). In addition, Pd catalyst can be deactivated by the formation of carbonaceous deposits, directly affecting the economy of the process. Physical separation by absorption using an organic solvent is an alternative commercial process used for the separation of acetylene [7]. Traditional organic absorbents, like N,N-dimethylformamide (DMF) and N-methylpyrrolidinone (NMP), present some typical disadvantages such as absorbent loss, difficult regeneration due to organic solvents' volatility and environmental pollution. For these reasons, big efforts have been focused on looking for new environmentally friendly solvents that overcome these disadvantages. In this sense, ionic liquids (ILs) have received attention as potential new solvents for gas separation processes [8]. The interest of using ILs to the task comes from their good properties: high and tunable solvent capacity, very low-vapor pressure, non-flammability, relatively high chemical and thermal stability and low corrosivity [8, 9]. An additional peculiarity of ILs is that they are known as "designer solvents" since the cation and anion can be modified/permuted to design an IL with specific properties for a particular application [10]. Therefore, all these properties make the ILs especially useful for gas absorption processes of compounds with different nature. Several groups have centered their research on the application of ILs as absorbents in different gas separation processes

[11-13] including several solutes as CO_2 [14-17], NH_3 [18-21] or volatile organic compounds (VOCs) [22, 23] (dimethylsulfide, toluene, etc.). Several experimental studies have demonstrated that ILs present a wide range of mass absorption capacity (of CO_2 [16, 24], NH_3 [20], VOCs [22, 23], etc.), depending on both their cation-anion chemical properties and molecular weights. In addition, it was reported that an important mass transfer kinetic control might occur in the absorption process using ILs [25], especially considering that these solvents present relatively high viscosity compared to conventional solvents. Indeed, it was found that thermodynamics and kinetics of CO_2 physical absorption in ILs do not always follow the same trends [16, 25]. Recently, experimental and theoretical studies on the separation of C_2H_2/C_2H_4 by ILs have also been reported [13, 26-30]. In those works, solubility measurements of acetylene in ILs of imidazolium or pyrrolidinium families with different anions have been carried out, obtaining higher capacities for acetylene absorption than those of traditional organic solvents [27]. It was experimentally demonstrated that the acetylene solubility increases in the IL with a stronger hydrogen-bond-acceptor (HBA) character [26, 27]. Molecular dynamics studies also investigated the behavior of acetylene-ILs mixtures, comparing the theoretical and experimental results [28, 29, 31]. In a recent study, Zhao et al [30] used the Conductor-like-Screening Model for Real Solvents (COSMO-RS) method to predict the Henry's constants of acetylene and ethylene in ILs. In general, it was concluded that ILs with hydrogen bond acceptor groups are promising candidates to selectively separate acetylene, at least from a thermodynamic point of view.

Recently, our group has developed a multiscale research strategy oriented to develop new gas capture processes based on ILs systems [22, 32, 33]. A detailed analysis –consisting on a three-stage methodology based on molecular simulation, experimental tests, and process simulation- is performed to select suitable ILs, alternative to organic solvents, for the separation of a specific gas solute. In the first stage, COSMO-RS a priori computational method [34] is applied to obtain a preliminary selection of ILs with favorable thermodynamic/kinetic properties for the absorption of the required solute, minimizing the long and difficult experimental studies. COSMO-RS has been widely used as computational tool for designing/selecting ILs with adequate properties for gas separation of CO_2, NH_3, Volatile Organic Compounds (VOCs), etc. since it provides reasonable predictions of gas-liquid equilibrium data [18, 20, 22, 32, 34-36]. The COSMO-RS method is applied to perform systematic screenings of Henry's law

constants of gas solutes in ILs, among a huge database of ions (more than 500), to evaluate the cation and anion effect on the gas-liquid equilibrium (GLE) of the system. In addition, COSMO-RS analysis allows understanding the GLE behavior of the systems in terms of the intermolecular interactions in the fluid mixture, providing a guide for the selection of ILs with improved characteristics for the task. In the second stage, experimental absorption tests are carried out at different temperatures and pressures; employing a high-pressure microbalance, with the aim of evaluating the thermodynamics and kinetics of gas absorption in ILs [14, 17, 25]. As a result, key parameters for the design of absorption columns at industrial scale are obtained, such as absorption capacities and diffusivities. In the last stage of multiscale research methodology, the gas separation processes based on ILs are modeled by using the Aspen Plus commercial process simulator, including both the absorption and solvent regeneration stages. For this purpose, an integrated COSMO-based/Aspen Plus approach is applied to create components that are not in Aspen's database, as it is the general case of ILs [35]. COSMO-RS or COSMO-SAC methods, available as COSMOSAC property model used in Aspen Plus, are used for the thermodynamic calculations in process simulations [35]. Once the ILs have been included in Aspen Plus's database, the individual separation operations and global processes involving ILs can be modeled, easily carrying out sensitivity analyses of different design variables [25, 37]. Our group has successfully applied this methodology to the study of the separation of aromatic-aliphatic hydrocarbon compounds by liquid-liquid extraction [37-39] and extractive distillation [39] using ILs, the regeneration of ILs by vacuum distillation [35], the absorption refrigeration cycles using ILs as absorbents [33], the toluene absorption with ILs [22] and the post-combustion CO_2 capture by physical absorption with ILs [25]. One main contribution of using process simulation analyses in the development of potential applications of ILs is that it allows introducing new technical and economic criteria in the selection of optimized ILs for specific separations. In addition, professional process simulators can be used to perform viability analyses of the technology based on ILs (through the estimation of energy consumptions, operating and capital cost, etc.) by comparison to available commercial technologies that use conventional solvents [25, 37]. For this reason, our group has developed an IL database (ILUAM) that includes 100 common ILs in four different databanks [40].

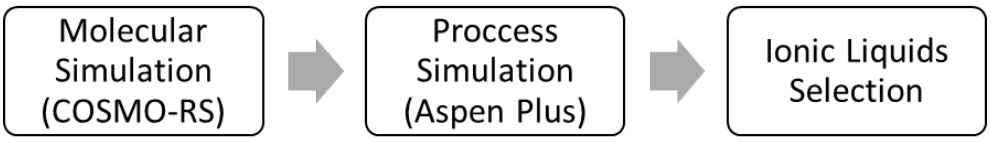

Figure 1: Alternative multiscale research strategy diagram

In this work, the potential application of ILs in the separation of acetylene by absorption is evaluated by means of COSMO-based/Aspen Plus multiscale research strategy. However, one main modification on above described multiscale methodology is introduced: in this study, both molecular and process simulation are firstly and sequentially applied (Figure 1) to preliminary select the ILs with better performance in the global gas separation processes. The use of the integrated molecular + process simulations allows performing a more rigorous selection of ILs from the view of the practical application at industrial scale, considering not only thermodynamic or kinetic properties but also technical, energetic and economic criteria. In addition, the performance of selected ILs is compared to that obtained using dimethylformamide (DMF), a conventional solvent industrially used to absorb acetylene. For this purpose, the COSMO-RS method is firstly applied to perform an IL property screening among a large database of ions (more than 300 ILs included). Henry's constant of acetylene in the IL solvent is predicted as thermodynamic parameter of reference to select ILs with high gas solute solubility, as it was successfully done previously [20, 22]. The COSMO-RS approach is also used to estimate the viscosities for the calculation of the diffusion coefficient of acetylene in the studied ILs, by using Wilke-Chang model; *i.e.,* molecular simulations also contribute to anticipating the kinetic behavior of the system. Additionally, COSMO-RS analysis allows better understanding the acetylene-IL mixture behavior from a molecular point of view, in terms of the intermolecular interactions happening in the fluid mixture. As a result, an initial selection of commercial ILs by means of thermodynamic and kinetic is carried out, comparing to the properties of DMF, which is used as benchmark industrial acetylene absorbent. Secondly, the unit operations for acetylene absorption and desorption are modeled using the selected ILs and DMF using the professional Aspen Plus process simulator. A sensitivity analysis of operating variables is carried out using rigorous equilibrium and rate-based models for the absorption operation in commercial packed columns, in order to evaluate the role of thermodynamics and kinetics in the separation efficiency. Lastly, the regeneration of the

exhausted solvent is studied with a flash distillation, analyzing, for each solvent used, the temperature and pressure effect on the product purity and solvent losses. Current computational analysis contributes as a preliminary evaluation of the potential application of IL for acetylene absorption, as an alternative to the DMF conventional solvent, providing a set of ILs with favorable absorbent properties, contributing to minimize the number of experimental tests needed at laboratory or pilot plant scale.

2. Computational Details

2.1 COSMO-RS calculations

Firstly, the geometry of gaseous compounds (acetylene and argon) involved in the work were optimized at BP86/TZVP computational level in gas phase. Two molecular models were used to describe de IL compounds: the ion-pair (CA) and the independent counter ions (C+A) models, optimizing the corresponding structures at BP86/TZVP computational level with solvent effect through the COSMO continuum solvation method. Once all the molecules were optimized until its minimum energy level, the polarized charge distribution on the molecular surface -obtained by a COSMO single point calculation- was saved in a .cosmo file. All these quantum-chemical calculations and .cosmo file generation were carried out in Turbomole 7.0 software. COSMOtherm program package (version C30_1501) and its parametrization BP_TZVP_C30_1501 was used, afterward, for the COSMO-RS calculations, obtaining the σ-profiles and σ-potentials of the pure compounds as well as the Henry's law constants of acetylene in ILs and detailed contributions to excess enthalpies in equimolar acetylene-IL mixtures. For the ILs case, a validation of Henry's law constants of different solutes employing both the CA and C+A models was carried out comparing calculated and experimentally measured Henry's law constants. The software employs the semiempirical Antoine equation for estimating the vapor pressure, which is used for the calculation of Henry's law constants by means of the following expression:

$$K_H = \gamma_i^{\infty} \cdot p_0^{vap} \quad (1)$$

Where K_H is Henry's law constant, γ_i^{∞} is the activity coefficient of the solute at infinite dilution in the IL calculated by COSMOtherm and p_0^{vap} is the vapor pressure of the pure gas, estimated by both COSMOtherm and the Antoine equation (obtained from reference [41]). A complete description of the procedure for the activity coefficient calculation could be found in the work developed by Klamt [42].

In order to accomplish the kinetic screening among the huge number of ionic liquids (more than 300), viscosities at 298.15 K were calculated by using COSMOtherm (full description in the Supplementary Information). The key kinetic parameter employed in our calculations is the diffusion coefficient (D). The widely used Wilke-Chang correlation [43] was used to estimate the diffusion coefficients of acetylene solute in ILs and DMF absorbent:

$$D = 7.4 \cdot 10^{-8} \cdot \frac{(\phi \cdot M_{IL})^{0.5} \cdot T}{\mu_{IL} \cdot V_{Acetylene}^{0.6}} \quad (2)$$

Where ϕ is the association parameter (with value of 1, considering in this case IL as unassociated solvent), M_{IL} is the molar weight of ILs, T is temperature (K), μ_{IL} is the viscosity of ILs (calculated by COSMOtherm with its later correction) and $V_{Acetylene}$ is the molar volume of acetylene at the corresponding temperature (calculated by COSMOtherm).

2.2 Component Definition and Property Model Specification in Aspen

In process simulation, the ILs are created as pseudo-components in Aspen Plus v8.8 using the ion-paired model (CA). For this purpose, molecular weight, normal boiling point and density (at 60 ºF) predicted by COSMO-RS were used to define IL as pseudo-component in Aspen Plus property system. In addition, to complete the component definition, the viscosity-to-temperature dependence was specified, using an Arrhenius type equation, employed by default in Aspen Plus. The experimental viscosity-to-temperature data was first regressed and then refined in a previous publication carried out by our group [44]. The gaseous compounds of the work (acetylene and argon) were included in the simulation as conventional compounds, and their parameters and properties were loaded from Aspen Plus database. The COSMOSAC property model was selected to estimate the activity coefficients of the components in mixture. There are three modifications of the property model: (i): the original COSMO-SAC model proposed by Lin and Sandler [45];(ii): the original COSMO-RS model proposed by Klamt [42]; and (iii): the modification to the Lin and Sandler model developed by P. Mathias et. al. The COSMOSAC property model in Aspen Plus needs the following additional molecular information of the compounds provided by COSMO-RS, required to complete the specifications of ILs, acetylene, and argon: molecular volumes (COSMO volume) and σ-

profiles. This information is included within the simulator in six parameters: CSACVL (compounds molecular volume in angstroms) and SGPRF1 to SGPRF5 (five sigma profile parameters, each containing 12 segments of the σ-profile). All the values related to the creation of the ILs as pseudo-components are included in Table S3 (Supplementary Information). More information on this computational approach was reported in the documentation of the ILUAM database, which will be soon published with information available for 100 common ILs [40].

2.3 Acetylene absorption

The acetylene absorption column was modeled using the *RADFRAC* model implemented in Aspen Plus v8.8, employing equilibrium and Rate-Based modes. The gas inlet was fed with an initial composition of 2 mol% of acetylene (typical composition studied in the literature [46, 47] between 0.5-3 mol%) and 98 mol % of argon and a constant gas flow of 10 kg/h (almost 100 L/min) (as reference for a pilot plant). Initially, the inlet temperature and pressure of the gas and absorbent streams were 40 ºC and 1 atm, respectively. Different simulation cases were developed to analyze the absorption stage: *Case 1:* The equilibrium column was simulated with one theoretical stage as reference varying the inlet liquid mass flow (L/G). As a result, acetylene recoveries for each selected IL were calculated as a function of the L/G ratio. *Case 2:* Using the equilibrium mode of RADFRAC column, the theoretical stage number was changed between 1-10 with the aim of estimating the needed liquid flow of absorbent for achieving 80% of acetylene recovery in each case. *Case 3:* Using the Rate-Based mode, the temperature of the gas and liquid inlets was varied from 293 to 363 K with the aim of studying the possible mass transfer limitations of the operation. For this purpose, it has been selected Raschig Rings packing (15-25 mm depending on column diameter) with a column height of 1 meter as a reference. The column diameter was calculated using the "Packing Sizing" utility of the RADFRAC column for a fractional approach to maximum capacity of 62% and then transferred to the "Packing Rating" utility of the RADFRAC model. The calculations provide different acetylene recovery as a function of the temperature. *Case 4:* Using the Rate-Based mode, different column designs (with Raschig Rings packing of 25 mm and a maximum capacity of 62%) were calculated fixing an acetylene recovery of 80 % when using ratio L/G ratio (in mass) in the range of 60-160, obtaining the needed diameter and height for the separation in each case.

The conditions for all the cases are summarized in Table 1:

Table 1: Conditions for the cases of study of the process simulation section

	Pressure (atm)	T (K)	G (kg/h)	L (kg/h)	Recovery	Mode	Stages
Case 1	1	313	10	10-1200	-	EQ	1
Case 2	1	313	10	-	80%	EQ	1 to 10
Case 3	1	293-393	10	100	-	EQ/RB	5/1m
Case 4	1	313	10	600-1600	80%	RB	-
Reg.	$1\text{-}10^{-5}$	313-393	-	-	-	-	-

2.4 Solvent regeneration

The regeneration unit was modeled using the *FLASH2* model implemented in Aspen Plus v8.8. The constant flow treated, which includes the absorbed gas in saturated DMF or IL, was 1300 kg/h, which was previously selected by modeling the absorption column that was inside the range of typical pilot plant columns (in terms of height/diameter ratio and pressure drop per meter of column). The regeneration was studied by decreasing the pressure at temperatures between 313 and 393 K. Thus, it could be analyzed the acetylene recovery and the acetylene purity of the clean gas stream.

3. Results

3.1 Molecular simulation: prediction of the interactions based on σ-profiles

COSMO-RS methodology calculates the thermodynamic properties of fluid mixtures using the molecular surface polarity distributions (σ-surface) of their individual compounds, obtained from quantum chemical calculations, which is easily visualized by the σ-profile histogram (σ-profile) [34]. Based on COSMO-RS theory, the σ-profile includes the main chemical information necessary to predict possible interactions of a compound in a fluid phase. Furthermore, COSMO-RS provides the σ-potential as an additional tool for analyzing the affinity of the solvent to interact with compounds that present charge density [μ (σ)] with polarity (σ). Figure 2 presents the σ-surface, σ-profile, and σ-potential of acetylene. Both, σ-profile and σ-potential can be qualitatively divided in three main regions upon the following cut-off values: hydrogen bond donor ($\sigma < -0.0082$ e/Å^2) and acceptor ($\sigma > +0.0082$ e/Å^2) regions and the non-polar region ($-0.0082 < \sigma > +0.0082$ e/Å^2). The σ-profile of acetylene is dominated by a series of peaks located in the non-polar region. Furthermore, the peak located at -0.012 e/Å^2, which corresponds

to the hydrogen atoms of acetylene molecule indicates their ability to act as hydrogen bond donor (acidic character). The σ-potential of acetylene reflects its strongly repulsive interactions with acidic groups. On the contrary, it presents weak attractive interactions with basic groups (hydrogen bond acceptor region of the histogram) and non-polar compounds.

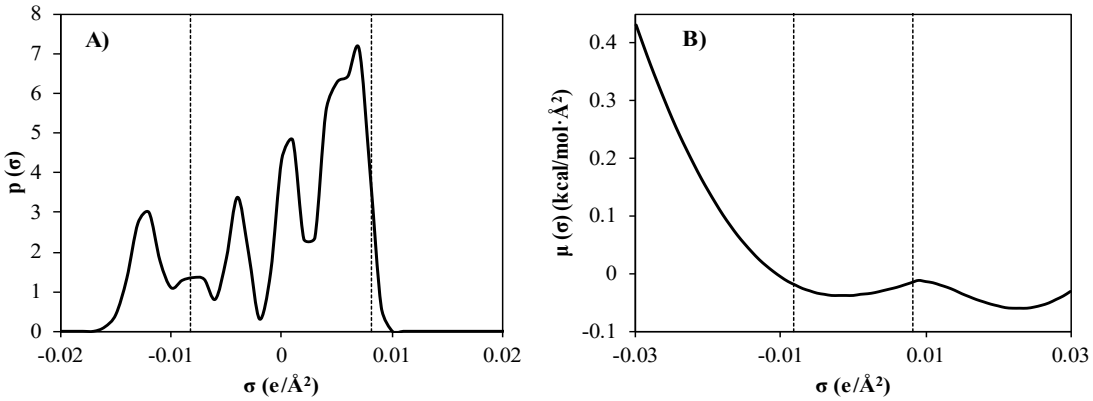

Figure 2: σ-profile and σ-potential of acetylene obtained by COSMO-RS

To anticipate the possible intermolecular interactions between acetylene and IL absorbents, σ-profiles and σ-potential of common anions (Figure 3) and cations (Figure 4) of common ILs are also analyzed. For instance, in the case of anions, the σ-profile of $[MeCOO]^-$ (Figure 3A) shows a main peak at the positive polar region (0.021 e/Å^2) which indicates a strong basic character (hydrogen bond acceptor) associated to the carboxylate oxygen atoms. These evidence can also be seen in the σ-potential in which high exothermic mixtures (strongly attractive interactions) are expected with acidic species and weak exothermic mixtures with non-polar compounds. The $[MeSO_3]^-$ anion shows a peak at 0.017 e/Å^2 due to the oxygen atoms, with also strong hydrogen bond acceptor character and some weak peaks at the non-polar region which corresponds to the methyl group and S atom. A similar description can be done for the $[MeSO_4]^-$ anion, but in this anion lower basic character is observed. In both cases, σ-potential indicates higher exothermic mixtures with acidic compounds than with non-polar compounds. The $[BF_4]^-$ anion shows a peak at 0.012 e/Å^2 which indicates a relatively weak hydrogen bond acceptor character, in agreement with its σ-potential curve. Lastly, the σ-profile related to $[NTf_2]^-$ anion presents its main peak at the non-polar region and an additional weaker peak at 0.01 e/Å^2, describing a big anion with low polarized charge and low basic character. In this case, the σ-potential indicates that high exothermic mixtures are not expected with acidic groups. Analyzing the σ-potential of common anions (Figure 3B),

repulsive interactions (endothermic mixtures) are expected when basic groups are involved in the operation. Due to the acidic character of acetylene, it is expected that better interaction will be accomplished using ILs with basic anions. In this sense, the basicity trend of anions would be $[MeCOO]^-$ > $[MeSO_3]^-$ > $[MeSO_4]^-$ > $[BF_4]^-$ > $[NTf_2]^-$.

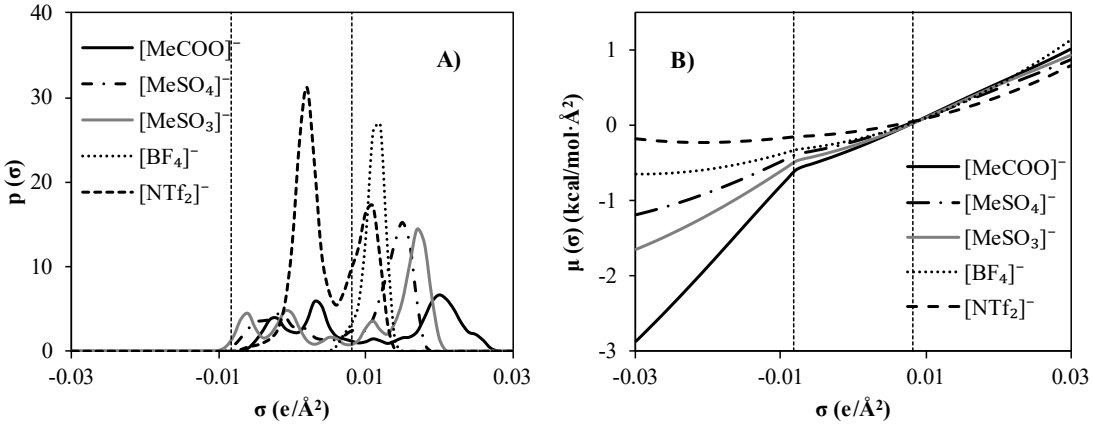

Figure 3: σ-profile and σ-potential of different anions obtained by COSMO-RS

The same analysis is carried out for common cations, in this sense, the σ-surfaces, σ-profiles, and σ-potentials of some studied cations can be seen in Figure 4. It is observed that the σ-profiles of cationic species are dominated by a main peak with an electronic density distribution in the non-polar region, corresponding to the alkyl substituents and the aromatic ($[bmim]^+$ and $[hxpy]^+$ cases) and aliphatic ($[N_{4444}]^+$ and $[P_{4444}]^+$ cases) head groups. In addition, for imidazolium cations as $[bmim]^+$, a weak peak is located at lower values than the cut off, -0.0082 e/Å^2, associated to the hydrogen atoms of the aromatic ring in $[bmim]^+$ case. A similar description may be done for pyridinium cations like $[hxpy]^+$ which presents a weak peak located at -0.011 e/ Å^2 corresponding to the hydrogen atoms of the aromatic ring. This indicates some acidic character of hydrogen atoms of imidazolium and pyridinium cations, stronger for the case of C_2-H. In order to complete this analysis, the σ-potential of cations is also evaluated (Figure 4B). From the results of the σ-potential, all the cations present repulsive interactions with acidic groups (as can be seen the endothermicity at the hydrogen bond donor region). In addition, some weak exothermic mixtures appear in the non-polar region. As studied above, $[bmim]^+$ and $[hxpy]^+$ cations may provide weak exothermic mixtures with compounds, present hydrogen bond acceptor groups. In fact, the hydrogen bond donor capacity of the cation families decreases in the following order: $[bmim]^+$ > $[hxpy]^+$ > $[P_{4444}]^+$ > $[N_{4444}]^+$. Therefore, looking for favorable acetylene-IL intermolecular interactions, it is expected that those cations with absence of acidic groups will be a better selection, since it may

avoid cation-anion hydrogen bond interactions, competing with acetylene-anion interactions.

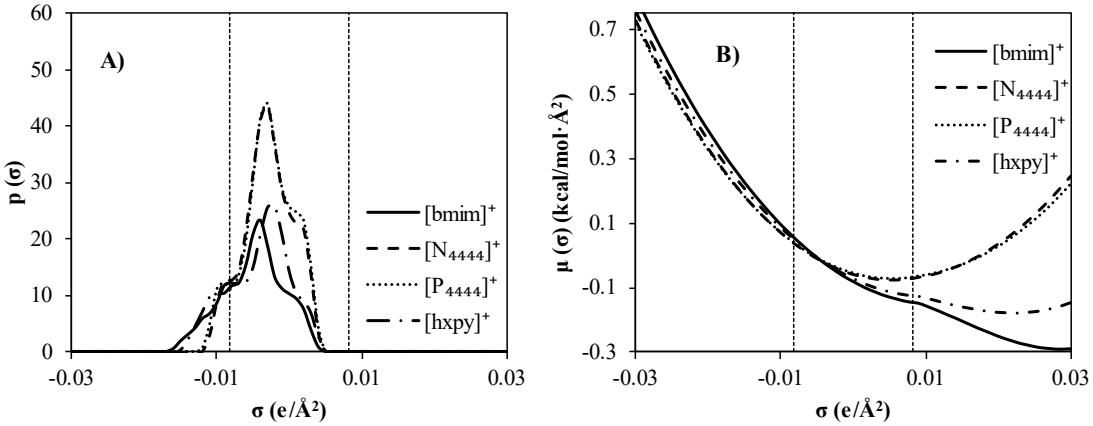

Figure 4: σ-profile and σ-potential of different cations obtained by COSMO-RS

3.2 Henry's law constants validation

Following, the capability of COSMO-RS to predict the gas solubility in ILs is evaluated by comparing experimental and calculated Henry constants ($K_H = \gamma_i^{\infty} \cdot p_i$) for more than 50 solute-IL systems collected in Gonzalez-Miquel's work [36] (including 11 solutes and 15 ILs), using both a molecular ion-paired model (CA) and an independent ions (C+A) model to simulate the IL solvent when experimental vapor pressure is employed and vapor pressure predicted by COSMO-RS is used. Compounds of very different nature such as CO_2, H_2, inert gases, aromatics, alkanes, alkenes and alkynes are included, involving a wide range of Henry's law constant values (from 0.1 bar for benzene in [hxmim][NTf_2] to 4500 bar for H_2 in [bmim][NTf_2]) at nearly room temperature. In order to assure the good predictions of Henry's law constants for acetylene, the available acetylene experimental vapor pressure values and their temperature dependence are included [41]. It is obtained that the best results are obtained (slope = 0.99, square correlation coefficient $R^2 = 0.98$) when experimental vapor pressure (p_i^*) and C+A model are used (Figure 5). However, it should be noted that COSMO-RS does not predict adequately the acetylene's vapor pressure ($p_i^*_{\text{COSMO-RS}} = 16.8$ bar, $p_i^*_{\text{experimental}} = 51.2$ bar at 300 K) when *.energy file is used. For this reason, experimental vapor pressure fitted to Antoine Equation was introduced by means of A, B and C coefficients which allows comparing the new Henry's law constants with experimental data. Figures that represent the rest of the cases are shown in Supplementary Material (Figures S2 and S3). The best results are obtained when experimental vapor pressures of acetylene are used, by

introducing the Antoine parameters in the *.vap file (A = 4.66; B = 909.08; C = 7.95) and C+A model will be used for next K_H calculations by COSMO-RS in this work.

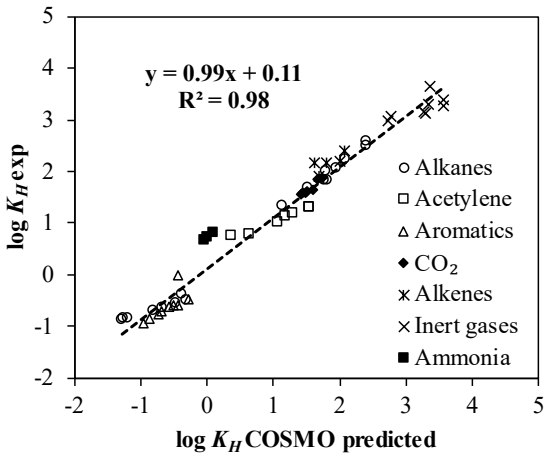

Figure 5: Experimental vs COSMO-RS Henry's law constants of solutes in ILs using experimental vapour pressure of the different solutes at near temperatures from 20-30ºC (C+A model).

3.3 Ionic Liquids Selection

Thermodynamic analysis. In order to select optimized ILs for acetylene absorption, COSMO-RS method was applied for predicting Henry's law constants (K_H) of acetylene in 306 LIs at 298.15 K. Hence, a computational screening was performed over ILs based on different cations and anions (see Table S1 in the Supplementary Material). The results from the COSMO-RS screening of Henry's law constants of acetylene in ILs (C+A model) are presented in Figure 6 (data available in Table S2 of the Supplementary Material). Firstly, it is concluded that suitable selection of ILs plays an important role in acetylene absorption, attending to the wide range of K_H (1-50 bar) for acetylene-IL systems obtained from COSMO-RS analysis. It is observed that the acetylene absorption capacity of ILs is more determined by the anion than by the cation, increasing the acetylene gas solubility in the IL solvent when increasing the hydrogen bond acceptor character of the anion, in good agreement with conclusions achieved from the σ-profiles and σ-potential of these species. Regarding the cation effect, tetra-substituted long chain phosphonium and ammonium cations seem to be the best selection for the task, followed by pyridinium and imidazolium cations. It is important to notice that ILs based on hydroxyl functionalized cations such as $[EtOHmim]^+$ or $[choline]^+$ are undesirable selections since the acetylene absorption capacity of IL decreases due to competitive hydrogen bond cation-anion interactions.

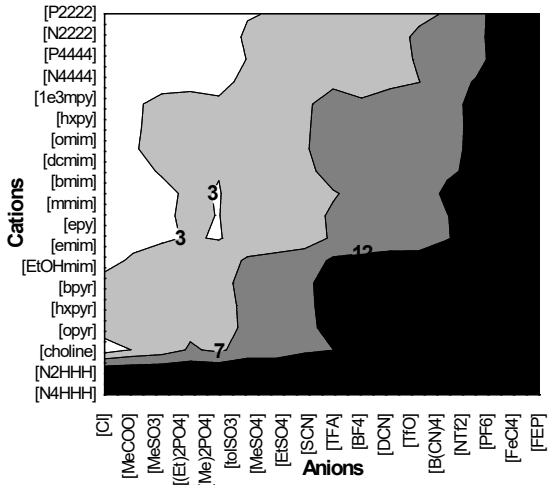

Figure 6: Screening of predicted Henry's law constants (bar) of acetylene in 306 ILs (C+A model using experimental vapor pressure) at T=298.15 K calculated by COSMO-RS

To obtain further insights on the absorption mechanism from a molecular point of view, COSMO-RS estimations of excess enthalpy (H^E) of acetylene-IL mixtures have been calculated to analyze the GLE data in terms of the intermolecular interactions in the liquid fluid, according to equation 1:

$$H^E = H^E(HB) + H^E(MF) + H^E(vdW) \quad (1)$$

Where excess enthalpies are obtained from hydrogen bonding (HB), electrostatic-misfit (MF) and van der Waals (vdW) contributions. Figure 7 compares H^E for equimolar acetylene-IL mixtures to Henry's law constant values at 298.15 K for 70 ILs calculated by COSMO-RS. As a general trend, higher solubility (decreasing K_H values) of acetylene in ILs is associated to higher exothermicity (decreasing H^E values) of the mixture, while the lower solubility of acetylene in the ILs is related with enthalpy values of the mixtures close to zero. Figure 8 allows analyzing the absorption of acetylene in a representative sample of ILs in terms of the contributions of different intermolecular interactions to the H^E values of acetylene-IL mixtures. It shows that a significant increase of the acetylene solubility in ILs with anions presenting a strong basic character, such as $[MeCOO]^-$ or $[MeSO_3]^-$, can be mainly ascribable to hydrogen bond interaction between acetylene solute and IL solvent. It is also noted that attractive electrostatic (MF) energies also contributes to the properties of the mixture, favoring the acetylene solubility in ILs.

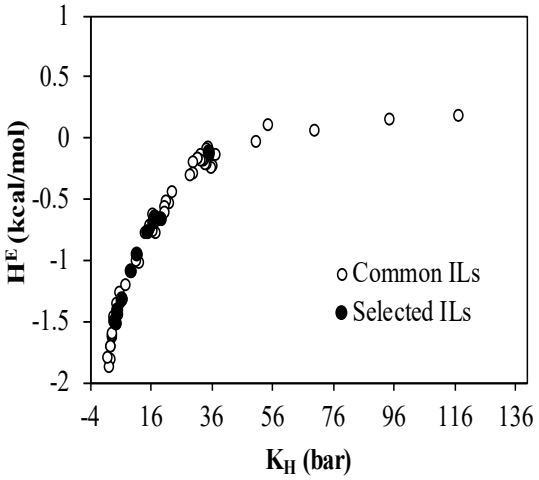

Figure 7: Excess molar enthalpies (H^E) of equimolar acetylene-IL mixtures versus Henry's law constants (K_H) for acetylene in 70 ILs (C+A model and experimental vapour pressure), both computed by COSMO-RS at 298.15 K

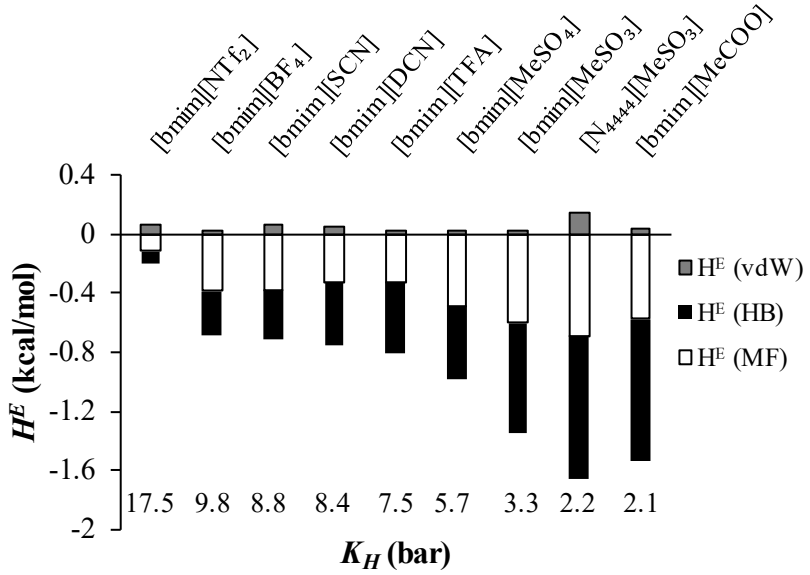

Figure 8: Description of the solvent effect on K_H of acetylene, at 298.15 K by using the interaction energies contributions [electrostatic (MF); Van der Waals (VdW); and hydrogen-bonding (HB)] to excess molar enthalpies of acetylene-IL (C+A model and experimental vapour pressure) mixture computed by COSMO-RS

Kinetic analysis. It is important to consider the relatively high values ILs viscosities and, correspondingly, their effect on the absorption rate. For this reason, Wilke-Chang correlation was applied in order to evaluate the diffusion coefficients of acetylene in ILs using the information computed by COSMO-RS. Therefore, in Figure 9, a computational screening of diffusion coefficients is performed for all the cations and anions involved in this work (data available in Table S3 of the Supplementary Material). As can be seen, the differences between diffusion coefficients of acetylene in different ILs are significant (up to two orders of magnitude), depending on these values on both the IL cation and anion. Therefore, it may be important to consider kinetic properties when selecting adequate ILs for the absorption of acetylene.

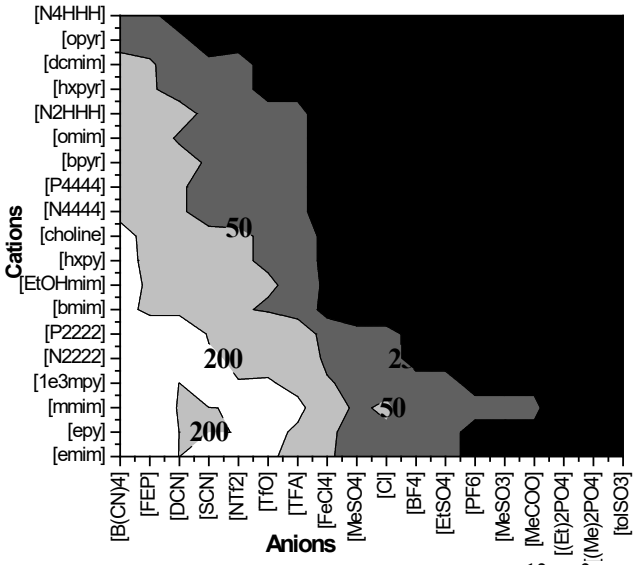

Figure 9: Screening of predicted diffusion coefficients (x10^{12} m^2/s) of acetylene in 306 ILs (C+A model) at T=313 K calculated by Wilke-Chang correlation

Analyzing the computational results, we preliminary select 9 commercial ILs, mainly attending to their favorable thermodynamic properties for acetylene absorption. This sample includes some ILs previously studied in the bibliography as a reference and others with low K_H values predicted by COSMO-RS (Table 2). As it has been noted, the selection of adequate ILs for a specific gas separation should also consider their transport properties. The ILs included in Table 2 present a wide range of molar weights, viscosities and consequently diffusivity values of acetylene in ILs.

Table 2: Properties of selected ILs/DMF or IL/DMF-acetylene system

ILs	MW	K_H (bar) 298.15 K	Mass Fraction 298.15 K, 1 atm	Viscosity (cP) 298.15 K	Diffusivity (m^2/s) 298.15 K
[bmim][NTf_2]	419.4	17.5	0.004	51.4 [44]	$4.1 \cdot 10^{-11}$
[bmim][BF_4]	226.0	9.8	0.013	114.2 [44]	$1.6 \cdot 10^{-11}$
[bmim][SCN]	197.3	8.8	0.017	55.7 [44]	$3.3 \cdot 10^{-11}$
[bmim][DCN]	205.3	8.4	0.017	31.1 [44]	$5.7 \cdot 10^{-11}$
[bmim][TFA]	252.2	7.5	0.016	77.5 [48]	$3.9 \cdot 10^{-11}$
[bmim][$MeSO_4$]	250.3	5.7	0.022	184.6 [44]	$8.7 \cdot 10^{-12}$
[bmim][$MeSO_3$]	234.3	3.3	0.047	713.1*	$8.5 \cdot 10^{-12}$
[N_{4444}][$MeSO_3$]	337.6	2.2	0.060	1560.7*	$1.8 \cdot 10^{-12}$
[bmim][MeCOO]	8.3	2.1	0.105	447.2 [44]	$3.5 \cdot 10^{-12}$
DMF	73.1	4.5	0.091	0.9 [49]	$1.5 \cdot 10^{-9}$

* Calculated by COSMO-RS

Analyzing the Table 2, it is observed that there are three ILs with Henry's law constants (in molar terms) of acetylene lower than DMF. Conversely, when the solubility is expressed in mass terms, only the [bmim][MeCOO] IL presents an acetylene solubility slightly higher than DMF. This is due to the high ILs molecular weight compared to DMF's. Regarding the kinetic properties, it is important to notice that DMF presents an acetylene diffusivity two or three order of magnitude higher than the selected ILs, because of its remarkably lower viscosity.

3.4 Process Simulation Results

GLE validation. Firstly, gas-liquid equilibria (GLE) calculations by COSMO-based/Aspen Plus approach were validated using experimental data collected from the literature. Calculations were carried out employing the three COSMO-based equations (codes 1-3) available in COSMOSAC property model as implicit in Aspen Plus (Table S4 of Supplementary Information). Attending relative mean deviations (MRD) when changing COSMOSAC models, COSMO-RS equation (code 2) reproduces better the GLE than the others two. Calculations performed using CA model to describe IL compounds provide better predictions of GLE for acetylene-IL systems (9 %) than those obtained using C+A model. The compared and calculated P-x diagram at 313 K for

acetylene-ILs systems involved in this work to the available experimental data [26] can be found in the Figure S4 of the Supplementary Material.

Acetylene absorption. The role of thermodynamics of acetylene absorption when using selected ILs and DMF absorbents was evaluated using RADFRAC column simulations in equilibrium model (*Case 1*). Figure 10 presents the acetylene recovery using different absorbent feed mass flows (different L/G) at fixed number of equilibrium stages (5). As expected, acetylene separation performance improves when increasing the solute solubility in ILs at fixed operating conditions (Table 2), observing that 3 ILs present solvent capabilities competitive with DMF from a thermodynamic standpoint. Thus, the ILs [bmim][MeCOO], [N_{4444}][$MeSO_3$] and [bmim][$MeSO_3$] allow reaching recoveries of more than 99 % in the modeled *Case 1*, similar than DMF; whereas a maximum acetylene recovery of 90% is obtained with the [bmim][$MeSO_4$] IL. The other ILs present lower separation efficiencies in the operating conditions of *Case 1*.

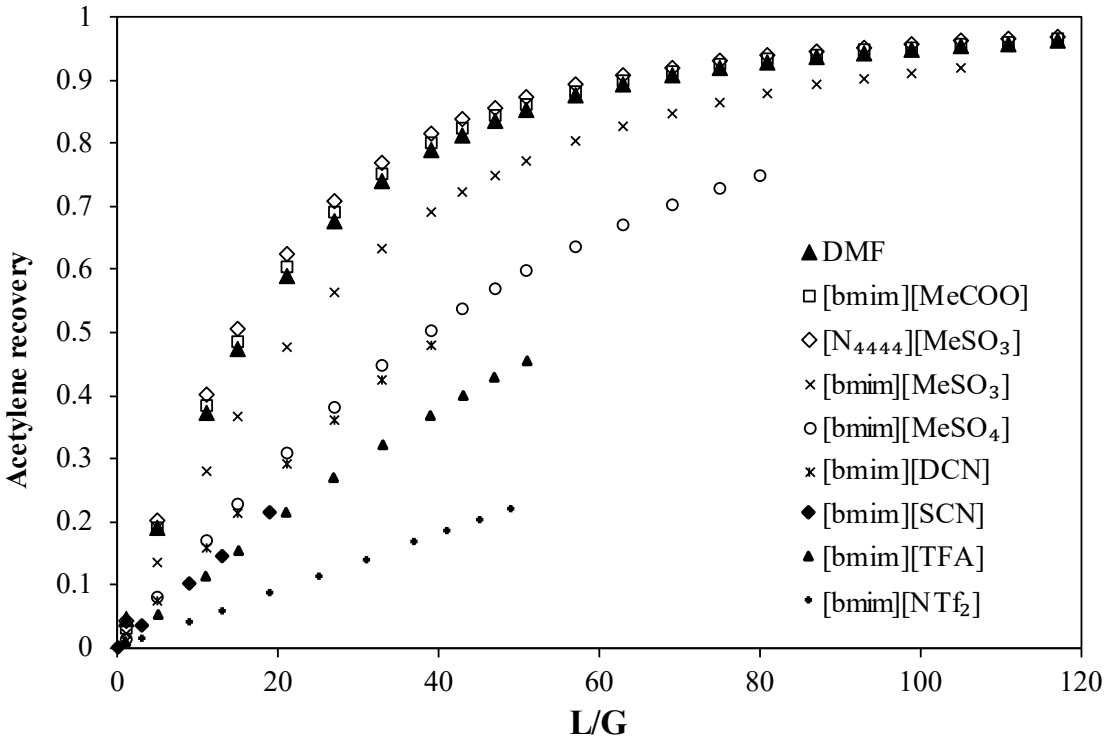

Figure 10: Acetylene recovery changing L/G ratio (in mass terms) using DMF and selected ILs, calculated using RADFRAC column in equilibrium mode (*Case 1*)

Case 2 simulations were carried out -using the 3 most favorable ILs and DMF- in order to evaluate liquid mass flow necessary (L/G) to achieve 80% acetylene recovery at different equilibrium stages (Figure 11). As can be seen, similar relationship between the number of equilibrium stages and needed L/G mass ratio for a specified separation is obtained for DMF and [bmim][MeCOO] and [N_{4444}][$MeSO_3$], whereas the IL [bmim][$MeSO_3$] shows slightly worse absorbent performance. The operating range was between 12-20 L/G ratio (Figure 11). For its good thermodynamic properties, [bmim][MeCOO] and [N_{4444}][$MeSO_3$] were selected for the next steps of the study.

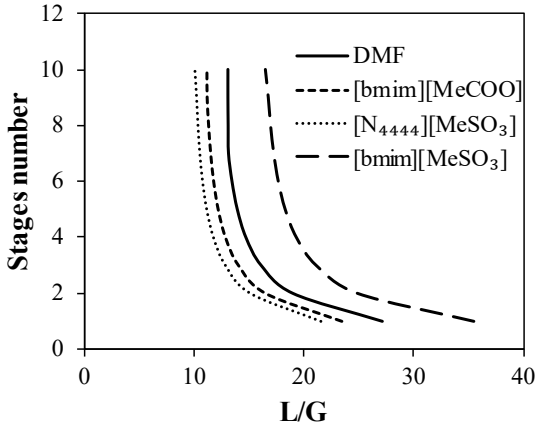

Figure 11: Mass liquid flow necessary for reaching 80 % acetylene recovery changing the stages number of the absorption column using DMF and 3 selected ILs, calculated using RADFRAC column in equilibrium mode (Case 2)

The potential kinetic control of acetylene absorption by ILs and DMF was evaluated modeling the absorption in a commercial packing column using the RADFRAC model in rate-based mode (*Case 3*). A L/G ratio of 10 was used since it allows obtaining a wide range of acetylene recoveries. Figures 12 compare the acetylene recovery obtained using Rate-Based and equilibrium modes of the RADFRAC column when the temperature of both the gas and liquid inlet streams is varied simultaneously from room temperature to 353 K. It can be observed that the acetylene absorption by ILs (Figure 12A and 12B) is clearly controlled by the mass transfer rate at near to room temperatures, reaching near a 50 % of recovery loss when equilibrium and Rate-Based modes are compared. On the contrary, the results obtained with the traditional organic solvent DMF (see Figure 12C), reflects just a 10 % of recovery loss, according to the short gap between equilibrium and Rate-Based curves. When the inlet temperature is increased, the kinetic control progressively diminishes until 333-343 K, temperature range where equilibrium

starts to control the process. This is directly related to the high viscosity of ILs at near room temperatures compared to traditional solvents such as DMF, difference that decreases at higher temperatures [44].

Figure 12: Acetylene recovery as a function of the gas and liquid inlet temperature when

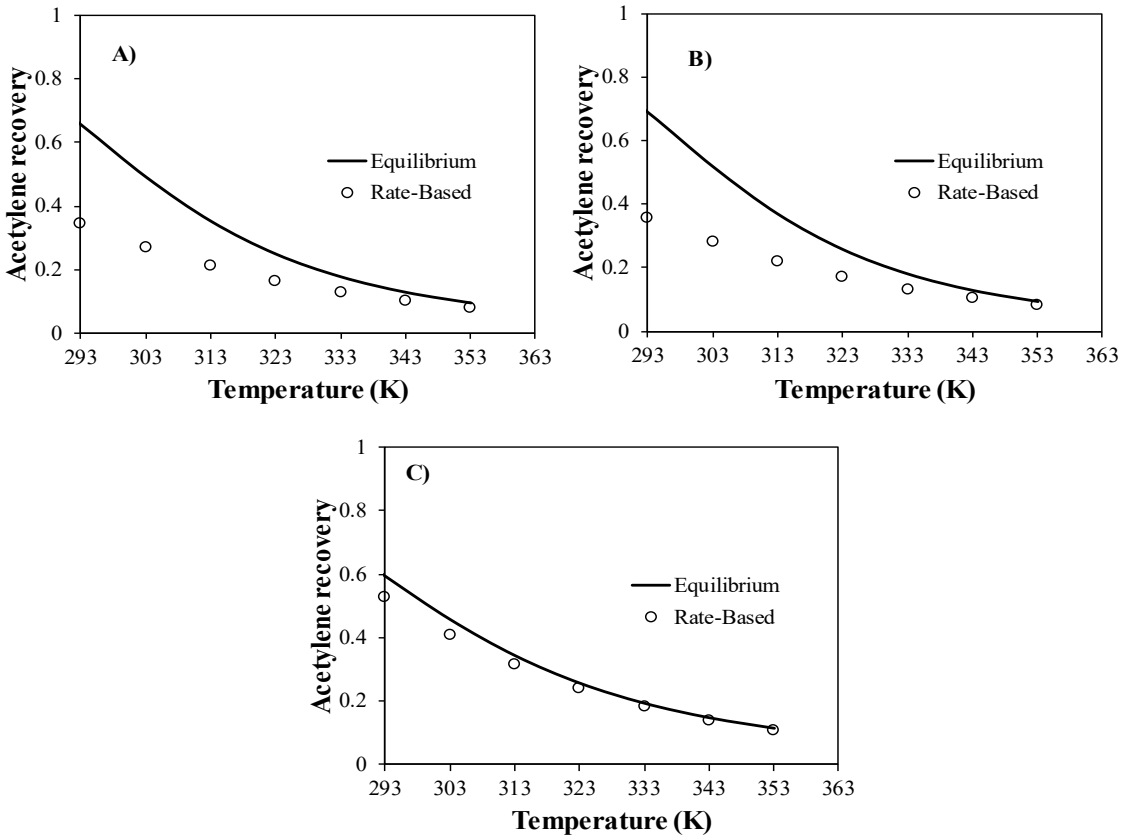

Rad-Frac model is operating in equilibrium and Rate-Based models for **A)** [bmim][MeCOO], **B)** [N_{4444}][$MeSO_3$], and **C)** DMF absorbents (Case 3)

Finally, simulations using Case 4 were performed to size the absorption column required to achieve a specific separation at fixed operating conditions (*Case 4*). Figure 13 presents the results of the column height needed to reach an 80% acetylene recovery when L/G ratio is varied from 60 to 160. As can be seen, remarkably higher packing column heights are required when using ILs (from 2-22 m) than when using DMF (0.5-2 m) at same operating conditions. In contrast, the diameter designed to fix a capacity factor of 62 % is similar for ILs and DMF, since it is mainly determined by L/G ratios at the fixed design specifications. Summarizing, the mass transfer rates play a crucial role in the

solvent performance of ILs in acetylene absorption, limiting their potential use as alternative to volatile organic solvents as DMF in the studied separation.

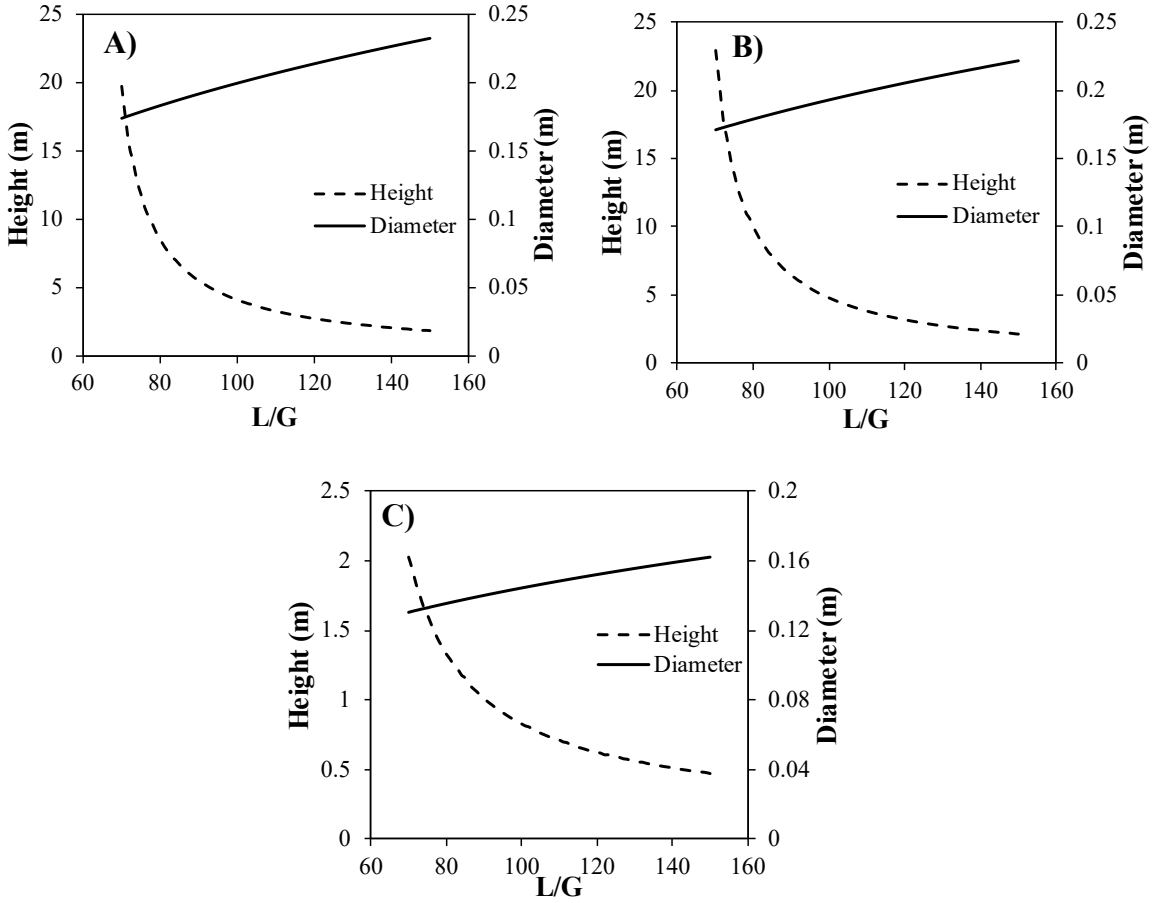

Figure 13: Absorption column design for different L/G ratios (in mass units) using **A)** [bmim][MeCOO], **B)** [N_{4444}][$MeSO_3$], and **C)** DMF as absorbents (Case 4)

Absorbent regeneration. Once evaluated the performance of ILs and DMF in absorption stage, it is also needed to simulate the regeneration unit of exhausted absorbent, since this later operation determines the operating costs of global acetylene separation processes [50]. For this purpose, a flash distillation by vacuum pressure with a temperature increase is proposed to regenerate the ILs and recovery the acetylene compound, based on previous results in the bibliography [25, 35, 51].

First, Figure 14A presents the acetylene recovery in the vapor stream at different operating pressures and temperatures when the IL is used as absorbent. As can be seen, when the temperature is increased and the pressure of the system is decreased, the highest acetylene recoveries are obtained. In fact, total acetylene recoveries were carried out at different conditions. The key parameter of the desorption operation seems to be the vacuum pressure required, reaching 100% acetylene recoveries from 10^{-3} atm. In addition,

in Figure 14B is shown the acetylene purity obtained. The data follow the same trend as the acetylene recovery one, reaching the maximum acetylene purity values when the vacuum pressure are minimum and the operation temperatures are maximum. Therefore, it has been demostrated the posibility of recovering the total amount of acetylene by a simple flash distillation by combining both a temperature increase and a pressure decrease.

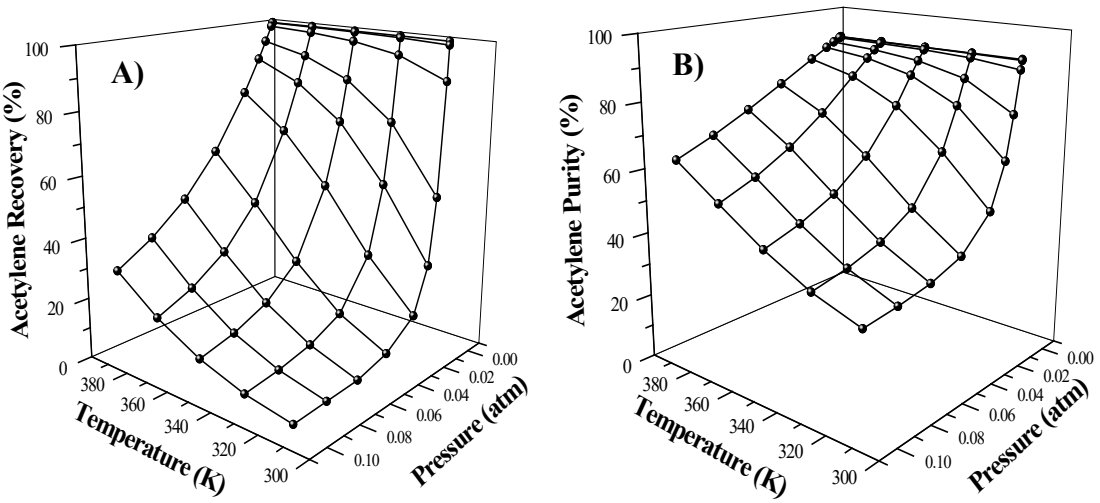

Figure 14: **A)** Acetylene recovery and **B)** Acetylene purity as a function of the temperature and pressure in the regenerator unit when IL is used

Second, Figure 15A shows the results of acetylene recovery for the DMF absorbent while Figure 15B analyzed the acetylene purity in the clean gas stream. The data follow the same trend as the IL case i.e. the maximum acetylene recoveries and purities are achieved for low values of pressure and high values of temperature. In this case, a wider range with total acetylene recovery than the IL case was found in different conditions. Nonetheless, when the acetylene recoveries are 100%, the acetylene purity of the clean gas stream is almost zero. This is directly atributed to the evaporation of the DMF solvent and the later loss in the vapor stream. In addition, if soft conditions are carried out in the regenerator, the maximum acetylene purity reached is 10% (clearly lower than the IL case in the same conditions). Therefore, a simple flash distillation operation cannot be used to regenerate the exhausted DMF absorbent without solvent loss, and much more costly multistage distillation is required. These results reveals a clear advantage of using ILs in the regeneration stage, since total acetylene recoveries and purities were reached by single stage distillation when ILs are employed.

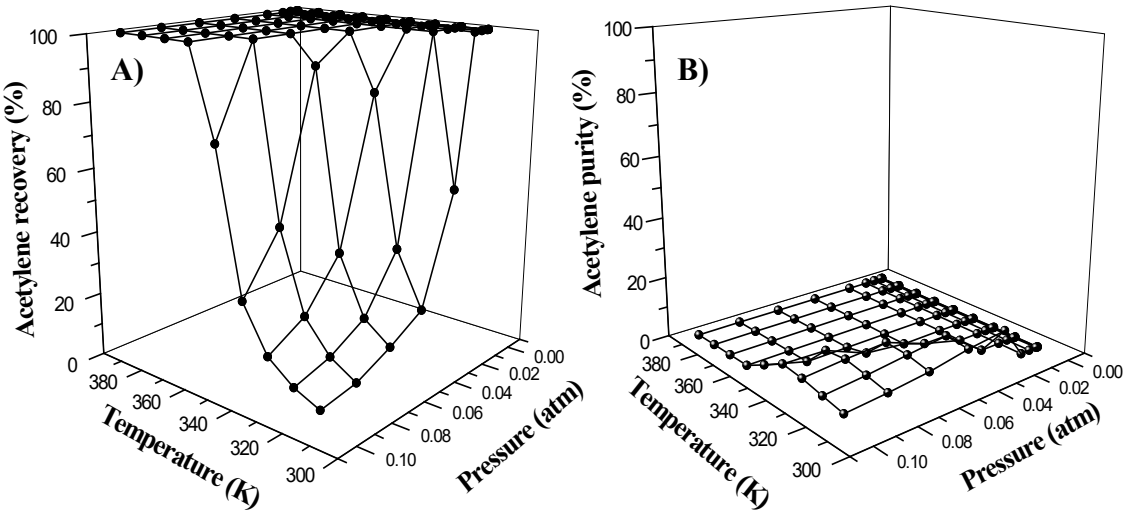

Figure 15: **A)** Acetylene recovery and **B)** Acetylene purity as a function of the temperature and pressure in the regenerator unit when DMF is used

Conclusions

In the present work, ILs were selected and evaluated for their potential application in acetylene absorption using a COSMO-based/Aspen Plus multiscale methodology. Molecular simulations were successfully carried out over a wide number of ILs in order to preliminary select a sample of absorbents with adequate thermodynamic and kinetic characteristics for such separation, competitive with those reported for conventional acetylene absorbents as DMF. It was observed a strong influence of the anion on the IL solvent properties, obtaining higher acetylene absorption capacity in ILs formed by anions with strong hydrogen bond acceptor character, due to the favorable solute-solvent interactions with acidic acetylene compound. In contrast, the diffusivity of acetylene in IL media is relatively low when comparing to the DMF case and it is observed that thermodynamics and mass transfer kinetics are strongly influenced by the selection of cation and anion. Then, the performance of ILs as acetylene absorbent was evaluated by modeling the absorption and IL regeneration units involved in the separation processes, using the Aspen Plus process simulator. From the thermodynamic point of view, at least two ILs are competitive with the DMF. However, when absorption operation is modeled in a more realistic scenario (commercial packed column, rigorous Rate-Based theoretical treatments), the acetylene absorption by selected ILs was found severely controlled by the mass transfer rate at near to room temperatures, in contrast to the case of DMF, whose absorption capacity is much properly exploited. Consequently, the necessary packing

height for reaching an 80% acetylene recovery is one order of magnitude greater than in DMF-based process. In contrast, the analysis of regeneration operation reveals the clear advantage of ILs as absorbent, since their depreciable volatility allows the efficient regeneration of the exhausted solvent and the acetylene recovery by using a simple flash distillation. On the contrary, using volatile DMF absorbent requires more energy demanding and costly distillation processes, in order to prevent the solvent loss through the gas stream. Current COSMO-based/Aspen Plus approach has been demonstrated useful to perform preliminary analysis of the potential application of ILs in new separation processes, providing relevant insights regarding the solvent selection and the viability of the new processes based on IL from comparison to conventional technologies, before starting with experimental essays, more cost and time demanding.

Acknowledgments

The authors are grateful to Comunidad Autónoma de Madrid (Project S2013/MAE-2800) and to Ministerio de Economía y Competitividad (MINECO) of Spain (Project CTQ2017-89441-R) for financial support. We are very grateful to Centro de Computación Científica de la Universidad Autónoma de Madrid for computational facilities.

References

1. Xia, T.F., J.F. Cai, H.Z. Wang, X. Duan, Y.J. Cui, Y. Yang, and G.D. Qian, *Microporous metal-organic frameworks with suitable pore spaces for acetylene storage and purification.* Microporous and Mesoporous Materials, 2015. **215**: p. 109-115.
2. Wang, X.X., J. Gao, J.S. Zhang, X.P. Zhang, and R.L. Guo, *Theoretical and Experimental Studies on Acetylene Absorption in a Polytetrafluoroethylene Hollow-Fiber Membrane Contactor.* Chemical Engineering & Technology, 2015. **38**(2): p. 215-222.
3. Sundaram, K.M., M.M. Shreehan, and E.F. Olszewski, *Ethylene*, in *Kirk-Othmer Encyclopedia of Chemical Technology*. 2000, John Wiley & Sons, Inc.
4. Huang, W., J.R. McCormick, R.F. Lobo, and J.G. Chen, *Selective hydrogenation of acetylene in the presence of ethylene on zeolite-supported bimetallic catalysts.* Journal of Catalysis, 2007. **246**(1): p. 40-51.
5. Lee, J.M., J. Palgunadi, J.H. Kim, S. Jung, Y.S. Choi, M. Cheong, and H.S. Kim, *Selective removal of acetylenes from olefin mixtures through specific physicochemical interactions of ionic liquids with acetylenes.* Physical Chemistry Chemical Physics, 2010. **12**(8): p. 1812-1816.
6. Ruta, M., G. Laurenczy, P.J. Dyson, and L. Kiwi-Minsker, *Pd nanoparticles in a supported ionic liquid phase: Highly stable catalysts for selective acetylene hydrogenation under*

continuous-flow conditions. Journal of Physical Chemistry C, 2008. **112**(46): p. 17814-17819.
7. Weissermel, K. and H.-J. Arpe, *Acetylene*, in *Industrial Organic Chemistry*. 2008, Wiley-VCH Verlag GmbH. p. 91-105.
8. Wilkes, J.S., P. Wasserscheid, and T. Welton, *Introduction*, in *Ionic Liquids in Synthesis*. 2008, Wiley-VCH Verlag GmbH & Co. KGaA. p. 1-6.
9. Huddleston, J.G., A.E. Visser, W.M. Reichert, H.D. Willauer, G.A. Broker, and R.D. Rogers, *Characterization and comparison of hydrophilic and hydrophobic room temperature ionic liquids incorporating the imidazolium cation.* Green Chemistry, 2001. **3**(4): p. 156-164.
10. Palomar, J., J.S. Torrecilla, J. Lemus, V.R. Ferro, and F. Rodriguez, *A COSMO-RS based guide to analyze/quantify the polarity of ionic liquids and their mixtures with organic cosolvents.* Physical Chemistry Chemical Physics, 2010. **12**(8): p. 1991-2000.
11. Han, D. and K.H. Row, *Recent Applications of Ionic Liquids in Separation Technology.* Molecules, 2010. **15**(4): p. 2405.
12. Han, X. and D.W. Armstrong, *Ionic Liquids in Separations.* Accounts of Chemical Research, 2007. **40**(11): p. 1079-1086.
13. Zhao, Y.S., R. Gani, R.M. Afzal, X.P. Zhang, and S.J. Zhang, *Ionic Liquids for Absorption and Separation of Gases: An Extensive Database and a Systematic Screening Method.* Aiche Journal, 2017. **63**(4): p. 1353-1367.
14. Moya, C., J. Palomar, M. Gonzalez-Miquel, J. Bedia, and F. Rodriguez, *Diffusion Coefficients of CO2 in Ionic Liquids Estimated by Gravimetry.* Industrial and Engineering Chemistry Research, 2014. **53**(35): p. 13782-13789.
15. Bara, J.E., T.K. Carlisle, C.J. Gabriel, D. Camper, A. Finotello, D.L. Gin, and R.D. Noble, *Guide to CO2 Separations in Imidazolium-Based Room-Temperature Ionic Liquids.* Industrial & Engineering Chemistry Research, 2009. **48**(6): p. 2739-2751.
16. Zeng, S., X. Zhang, L. Bai, X. Zhang, H. Wang, J. Wang, D. Bao, M. Li, X. Liu, and S. Zhang, *Ionic-Liquid-Based CO2 Capture Systems: Structure, Interaction and Process.* Chemical Reviews, 2017. **117**(14): p. 9625-9673.
17. Moya, C., N. Alonso-Morales, M.A. Gilarranz, J.J. Rodriguez, and J. Palomar, *Encapsulated Ionic Liquids for CO2 Capture: Using 1-Butyl-methylimidazolium Acetate for Quick and Reversible CO2 Chemical Absorption.* ChemPhysChem, 2016. **17**(23): p. 3891-3899.
18. Palomar, J., M. Gonzalez-Miquel, J. Bedia, F. Rodriguez, and J.J. Rodriguez, *Task-specific ionic liquids for efficient ammonia absorption.* Separation and Purification Technology, 2011. **82**(1): p. 43-52.
19. Yokozeki, A. and M.B. Shiflett, *Ammonia Solubilities in Room-Temperature Ionic Liquids.* Industrial & Engineering Chemistry Research, 2007. **46**(5): p. 1605-1610.
20. Bedia, J., J. Palomar, M. Gonzalez-Miquel, F. Rodriguez, and J.J. Rodriguez, *Screening ionic liquids as suitable ammonia absorbents on the basis of thermodynamic and kinetic analysis.* Separation and Purification Technology, 2012. **95**: p. 188-195.
21. Lemus, J., J. Bedia, C. Moya, N. Alonso-Morales, M.A. Gilarranz, J. Palomar, and J.J. Rodriguez, *Ammonia capture from the gas phase by encapsulated ionic liquids (ENILs).* Rsc Advances, 2016. **6**(66): p. 61650-61660.
22. Bedia, J., E. Ruiz, J. de Riva, V.R. Ferro, J. Palomar, and J.J. Rodriguez, *Optimized ionic liquids for toluene absorption.* AIChE Journal, 2013. **59**(5): p. 1648-1656.
23. Salar-Garcia, M.J., V.M. Ortiz-Martinez, F.J. Hernandez-Fernandez, A.P. de los Rios, and J. Quesada-Medina, *Ionic liquid technology to recover volatile organic compounds (VOCs).* Journal of Hazardous Materials, 2017. **321**: p. 484-499.
24. Babamohammadi, S., A. Shamiri, and M.K. Aroua, *A review of CO2 capture by absorption in ionic liquid-based solvents.* Reviews in Chemical Engineering, 2015. **31**(4): p. 383-412.

25. de Riva, J., J. Suarez-Reyes, D. Moreno, I. Diaz, and V. Ferro, *Ionic liquids for post-combustion CO 2 capture by physical absorption: Thermodynamic, kinetic and process analysis.* International journal of greenhouse gas control, 2017. **61**: p. 61-70.
26. Palgunadi, J., H.S. Kim, J.M. Lee, and S. Jung, *Ionic liquids for acetylene and ethylene separation: Material selection and solubility investigation.* Chemical Engineering and Processing: Process Intensification, 2010. **49**(2): p. 192-198.
27. Palgunadi, J., S.Y. Hong, J.K. Lee, H. Lee, S.D. Lee, M. Cheong, and H.S. Kim, *Correlation between Hydrogen Bond Basicity and Acetylene Solubility in Room Temperature Ionic Liquids.* Journal of Physical Chemistry B, 2011. **115**(5): p. 1067-1074.
28. Xu, H., Z. Han, D.J. Zhang, and J.H. Zhan, *Interface Behaviors of Acetylene and Ethylene Molecules with 1-Butyl-3-methylimidazolium Acetate Ionic Liquid: A Combined Quantum Chemistry Calculation and Molecular Dynamics Simulation Study.* Acs Applied Materials & Interfaces, 2012. **4**(12): p. 6646-6653.
29. Zhao, X., H.B. Xing, Q.W. Yang, R.L. Li, B.G. Su, Z.B. Bao, Y.W. Yang, and Q.L. Ren, *Differential Solubility of Ethylene and Acetylene in Room-Temperature Ionic Liquids: A Theoretical Study.* Journal of Physical Chemistry B, 2012. **116**(13): p. 3944-3953.
30. Zhao, X., Q. Yang, D. Xu, Z. Bao, Y. Zhang, B. Su, Q. Ren, and H. Xing, *Design and screening of ionic liquids for C2H2/C2H4 separation by COSMO-RS and experiments.* AIChE Journal, 2015. **61**(6): p. 2016-2027.
31. Xing, H., X. Zhao, Q. Yang, B. Su, Z. Bao, Y. Yang, and Q. Ren, *Molecular dynamics simulation study on the absorption of ethylene and acetylene in ionic liquids.* Industrial and Engineering Chemistry Research, 2013. **52**(26): p. 9308-9316.
32. Ferro, V.R., E. Ruiz, M. Tobajas, and J.F. Palomar, *Integration of COSMO-based methodologies into commercial process simulators: Separation and purification of reuterin.* Aiche Journal, 2012. **58**(11): p. 3404-3415.
33. Ruiz, E., V.R. Ferro, J. de Riva, D. Moreno, and J. Palomar, *Evaluation of ionic liquids as absorbents for ammonia absorption refrigeration cycles using COSMO-based process simulations.* Applied Energy, 2014. **123**: p. 281-291.
34. Klamt, A., F. Eckert, and W. Arlt, *COSMO-RS: An Alternative to Simulation for Calculating Thermodynamic Properties of Liquid Mixtures*, in *Annual Review of Chemical and Biomolecular Engineering, Vol 1*, J.M. Prausnitz, M.F. Doherty, and R.A. Segalman, Editors. 2010, Annual Reviews: Palo Alto. p. 101-122.
35. Ferro, V.R., E. Ruiz, J. de Riva, and J. Palomar, *Introducing process simulation in ionic liquids design/selection for separation processes based on operational and economic criteria through the example of their regeneration.* Separation and Purification Technology, 2012. **97**: p. 195-204.
36. Gonzalez-Miquel, M., J. Palomar, and F. Rodriguez, *Selection of ionic liquids for enhancing the gas solubility of volatile organic compounds.* Journal of Physical Chemistry B, 2013. **117**(1): p. 296-306.
37. de Riva, J., V.R. Ferro, D. Moreno, I. Diaz, and J. Palomar, *Aspen Plus supported conceptual design of the aromatic-aliphatic separation from low aromatic content naphtha using 4-methyl-N-butylpyridinium tetrafluoroborate ionic liquid.* Fuel Processing Technology, 2016. **146**: p. 29-38.
38. Ferro, V.R., J. de Riva, D. Sanchez, E. Ruiz, and J. Palomar, *Conceptual design of unit operations to separate aromatic hydrocarbons from naphtha using ionic liquids. COSMO-based process simulations with multi-component "real" mixture feed.* Chemical Engineering Research & Design, 2015. **94**: p. 632-647.
39. Diaz, I., J. Palomar, M. Rodriguez, J. de Riva, V. Ferro, and E.J. Gonzalez, *Ionic liquids as entrainers for the separation of aromatic-aliphatic hydrocarbon mixtures by extractive distillation.* Chemical Engineering Research & Design, 2016. **115**: p. 382-393.
40. Ferro, V.R., C. Moya, D. Moreno, R. Santiago, J. de Riva, G. Pedrosa, M. Larriba, I. Diaz, and J. Palomar, *Enterprise Ionic Liquids Database (ILUAM) for Use in Aspen ONE*

Programs Suite with COSMO-Based Property Methods. Industrial & Engineering Chemistry Research, 2018. **57**(3): p. 980-989.
41. Ambrose, D. and R. Townsend, *Vapour pressure of acetylene.* Transactions of the Faraday Society, 1964. **60**(0): p. 1025-1029.
42. Klamt, A., *Conductor-like Screening Model for Real Solvents: A New Approach to the Quantitative Calculation of Solvation Phenomena.* The Journal of Physical Chemistry, 1995. **99**(7): p. 2224-2235.
43. Wilke, C.R. and P. Chang, *CORRELATION OF DIFFUSION COEFFICIENTS IN DILUTE SOLUTIONS.* Aiche Journal, 1955. **1**(2): p. 264-270.
44. de Riva, J., V.R. Ferro, L. del Olmo, E. Ruiz, R. Lopez, and J. Palomar, *Statistical Refinement and Fitting of Experimental Viscosity-to-Temperature Data in Ionic Liquids.* Industrial & Engineering Chemistry Research, 2014. **53**(25): p. 10475-10484.
45. Lin, S.-T. and S.I. Sandler, *A Priori Phase Equilibrium Prediction from a Segment Contribution Solvation Model.* Industrial & Engineering Chemistry Research, 2002. **41**(5): p. 899-913.
46. McCue, A.J., A. Guerrero-Ruiz, C. Ramirez-Barria, I. Rodriguez-Ramos, and J.A. Anderson, *Selective hydrogenation of mixed alkyne/alkene streams at elevated pressure over a palladium sulfide catalyst.* Journal of Catalysis, 2017. **355**: p. 40-52.
47. Kuhn, M., M. Lucas, and P. Claus, *Precise recognition of catalyst deactivation during acetylene hydrogenation studied with the advanced TEMKIN reactor.* Catalysis Communications, 2015. **72**: p. 170-173.
48. Li, W., Z. Zhang, B. Han, S. Hu, Y. Xie, and G. Yang, *Effect of Water and Organic Solvents on the Ionic Dissociation of Ionic Liquids.* The Journal of Physical Chemistry B, 2007. **111**(23): p. 6452-6456.
49. NIST, *Ionic Liquids Database - (ILThermo).* 2013.
50. Pässler, P., W. Hefner, K. Buckl, H. Meinass, A. Meiswinkel, H.-J. Wernicke, G. Ebersberg, R. Müller, J. Bässler, H. Behringer, and D. Mayer, *Acetylene*, in *Ullmann's Encyclopedia of Industrial Chemistry*. 2000, Wiley-VCH Verlag GmbH & Co. KGaA.
51. Larriba, M., J. de Riva, P. Navarro, D. Moreno, N. Delgado-Mellado, J. Garcia, V.R. Ferro, F. Rodriguez, and J. Palomar, *COSMO-based/Aspen Plus process simulation of the aromatic extraction from pyrolysis gasoline using the 1 4empy NTf2 + emim DCA } ionic liquid mixture.* Separation and Purification Technology, 2018. **190**: p. 211-227.